

date	10/23/2002	ref.	TOS-MMO/2002/389	page	1/17
from	Robert J. Daddato, TOS-MMO		visa		
To	Georges Gourmelon, EOP-PTE		copy	Dominic Doyle, TOS-MMO, Bernhard Furch, TOS-MMO, laboratory file	
Subject	Reflected wavefront measurement of Cryosat LRR module				

Technical Memo

1. Scope of this Technical Memo

This memo presents the results of reflected wavefront measurements of the seven fused silica corner cubes of the Cryosat-LRR-01 retroreflector module. The measurements were carried out with the ZYGO Mark GPI Fizeau interferometer in the Optics Section cleanroom, in support of the Cryosat project.

A repeat measurement was carried out after vibration testing in order to determine whether the corner cubes had sustained damage.

2. Test set-up and measurement procedure

The reflected wavefront was measured in double pass at 632.8 nm with a commercial ZYGO Mark GPI Fizeau type phase shifting interferometer used for routine measurements at the ESTEC optics laboratory. Instrument control, data acquisition and analysis is automatically handled by the ZYGO Metro Pro software. For these double pass measurements the GPI Corner Cube application was used. The measurement cavity for the measurements in double pass is effectively formed by the front surface of the 4" transmission flat (ZYGO), with the retroreflector samples measured in double pass transmission inside the cavity.

The magnification was adjusted with the internal optical 1 - 6 x zoom, in order to fill the camera image as completely as possible.

The individual corner cubes are numbered 1 - 7 for identification, the numbering being indicated in figure 1 below. For the measurements the corner cubes were oriented with one facet edge (one edge most closely pointing towards the apex of the module) in vertical alignment with the ZYGO measurement reticle. The central cube was measured in the orientation indicated in figure 1.

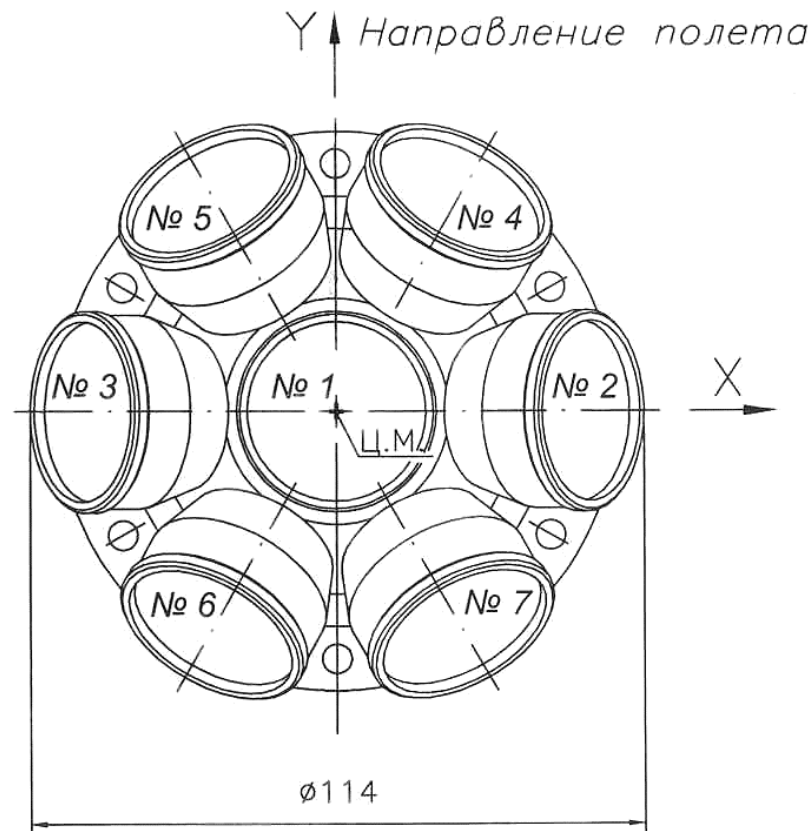


Fig. 1: Geometry of Cryosat-LRR-01

The refractive index of fused silica is $n = 1.4579 @ 633 \text{ nm}$. Since the material - and hence the refractive index - were not known at the time of the measurements made prior to vibration testing, an assumed refractive index of 1.5 was entered into the ZYGO software. The calculated dihedral angular errors and beam deviations indicated in the appended measurement protocols should therefore be ignored for the measurements carried out before vibration testing.

The ZYGO measurement protocols are appended as Figs. 1 - 14, the PV and RMS values are summarized in the table below.

3. Measurement result summary (transmitted wavefront error at 632.8 nm)

Corner cube no.	Date of measurement	PV [λ]	RMS [λ]	Comments	Fig.
1	2002-09-27	0.96	0.21	before vibration test	1
	2002-10-22	1.02	0.20	after vibration test	2
2	2002-09-29	0.91	0.18	before vibration test	3
	2002-10-22	0.81	0.17	after vibration test	4
3	2002-09-29	0.73	0.16	before vibration test	5
	2002-10-22	0.66	0.15	after vibration test	6
4	2002-09-29	0.73	0.15	before vibration test	7
	2002-10-22	0.71	0.15	after vibration test	8
5	2002-09-29	0.87	0.16	before vibration test	9
	2002-10-22	0.79	0.16	after vibration test	10
6	2002-09-29	0.84	0.18	before vibration test	11
	2002-10-22	0.84	0.16	after vibration test	12
7	2002-09-29	0.83	0.17	before vibration test	13
	2002-10-22	0.77	0.17	after vibration test	14

The differences in the RMS values prior to and after the vibration testing are in every case not larger than $\lambda / 100$ and therefore within the measurement uncertainty. The optical performance of the corner cubes has not been affected by the vibration test.

4. Figures

The printouts of the ZYGO MetroPro measurement protocols are appended.

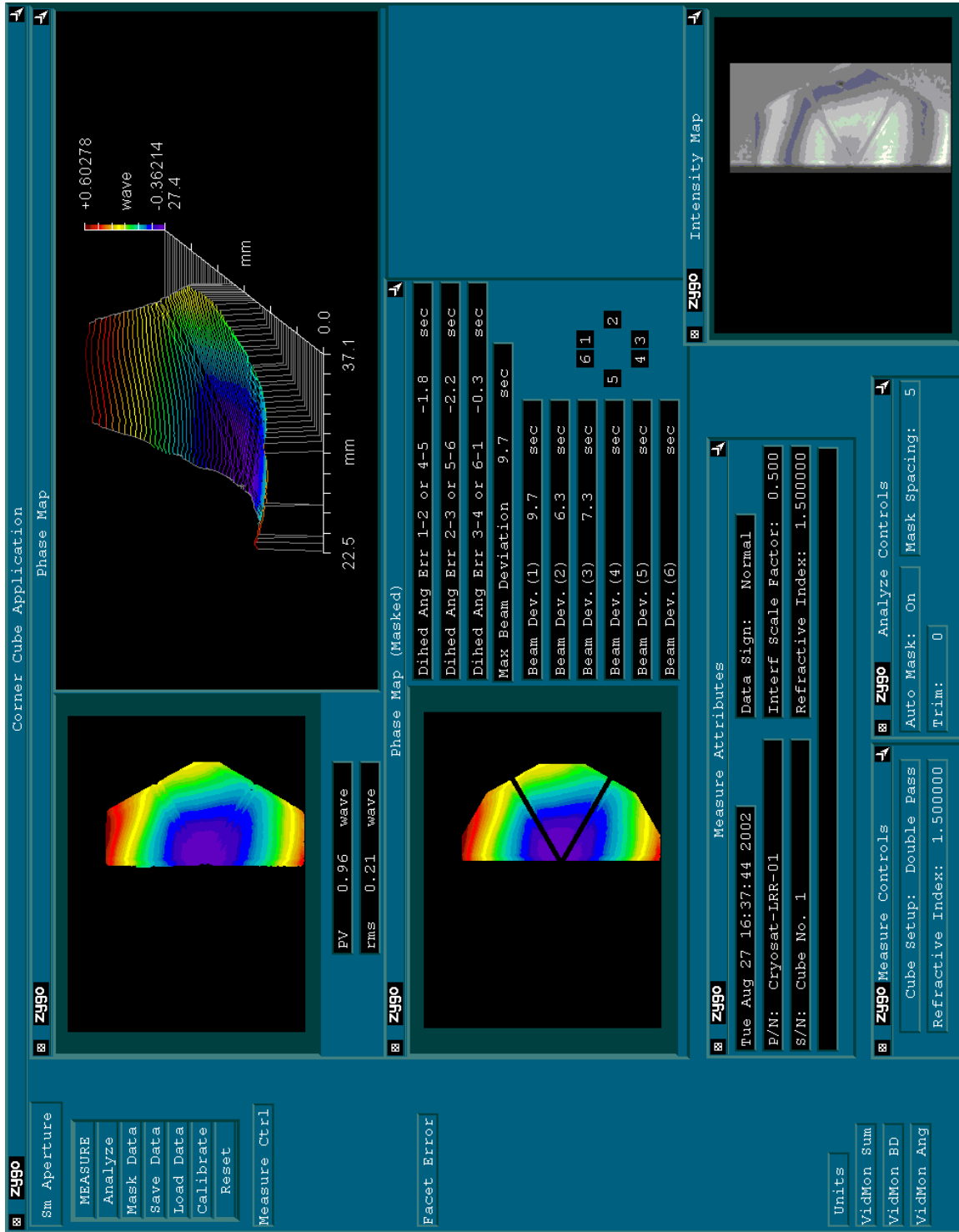


Fig. 2: Cryosat-LRR-01, cube #1, before vibration test

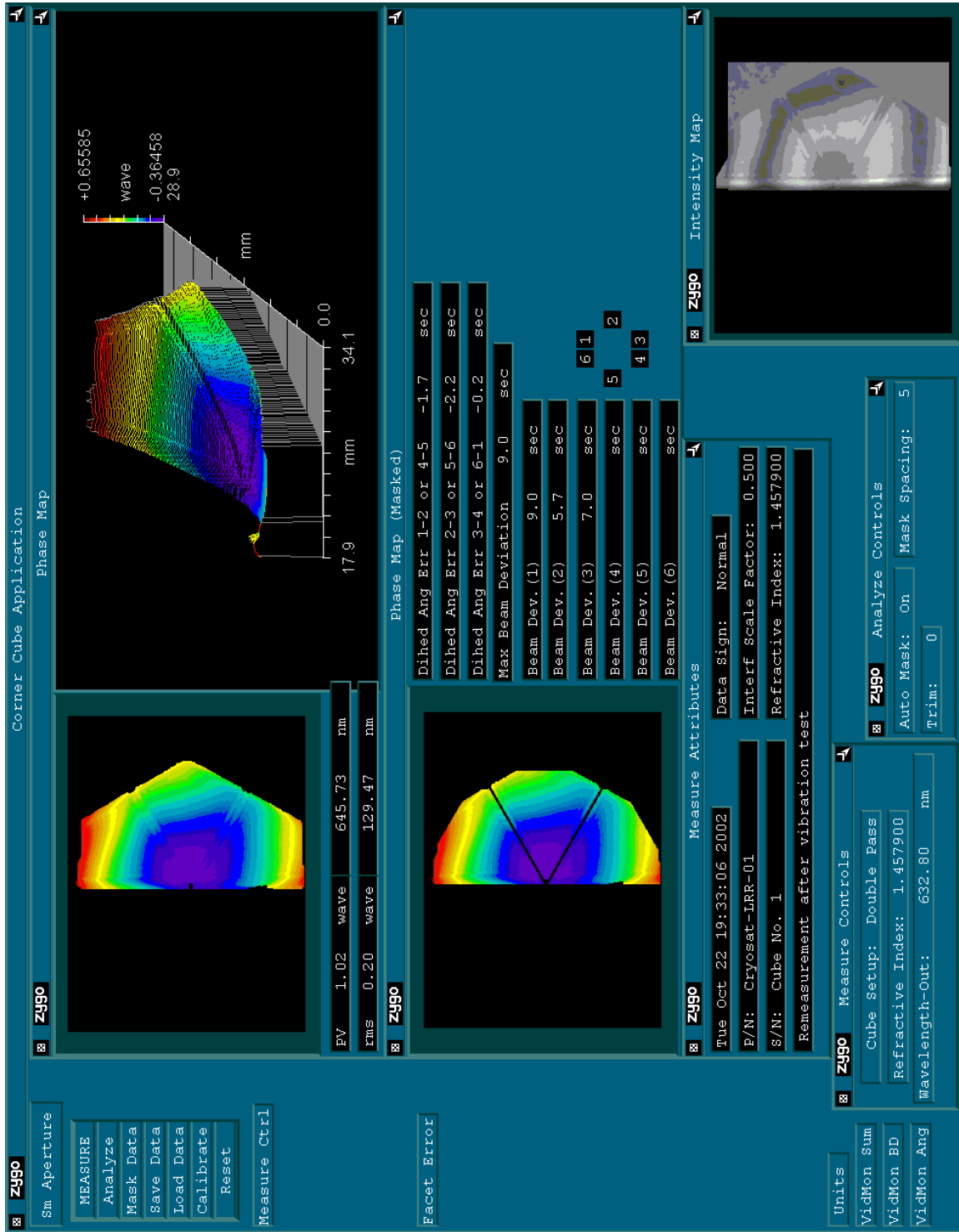


Fig. 3: Cryosat-LRR-01, cube #1, after vibration test

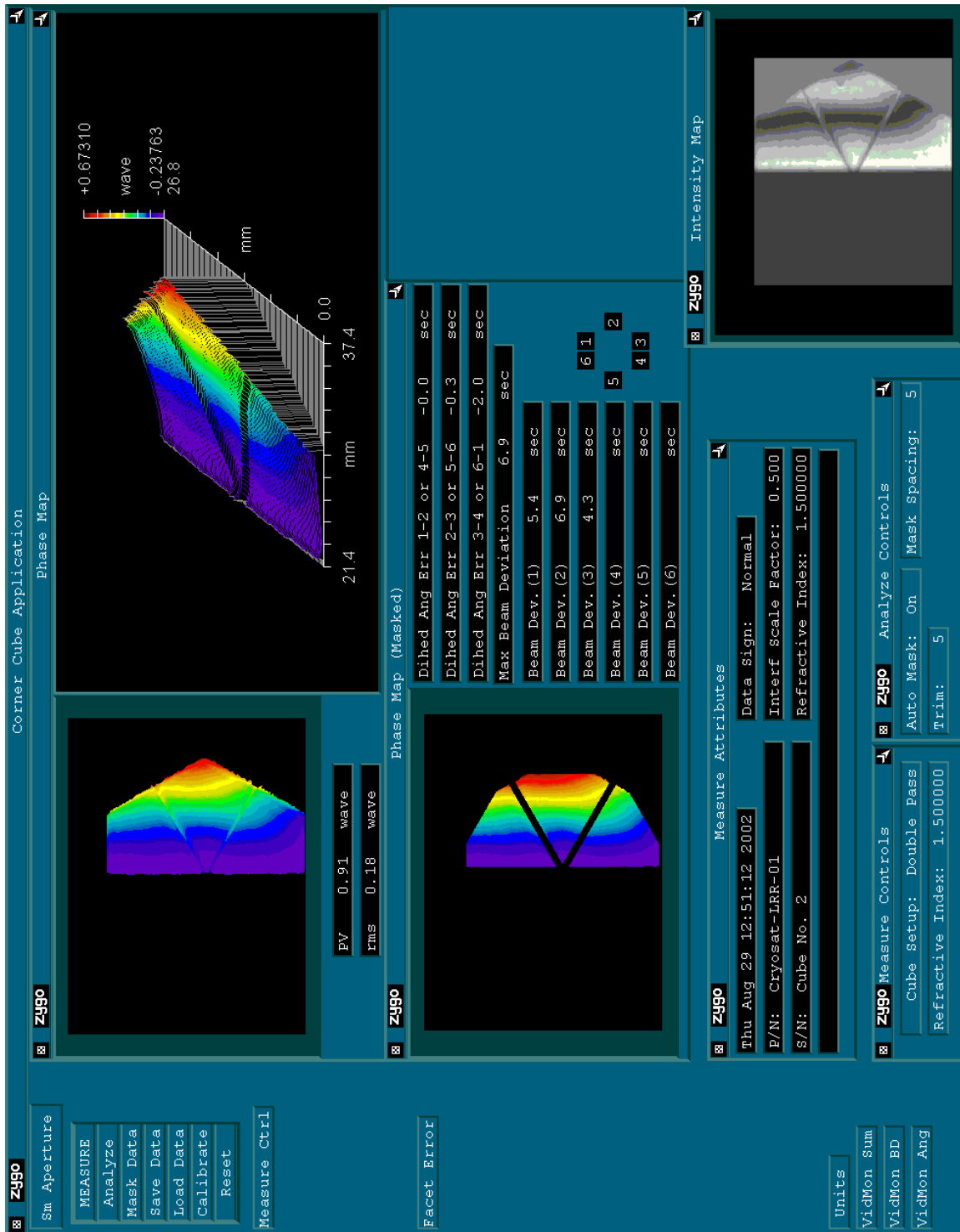


Fig. 4: Cryosat-LRR-01, cube #2, before vibration test

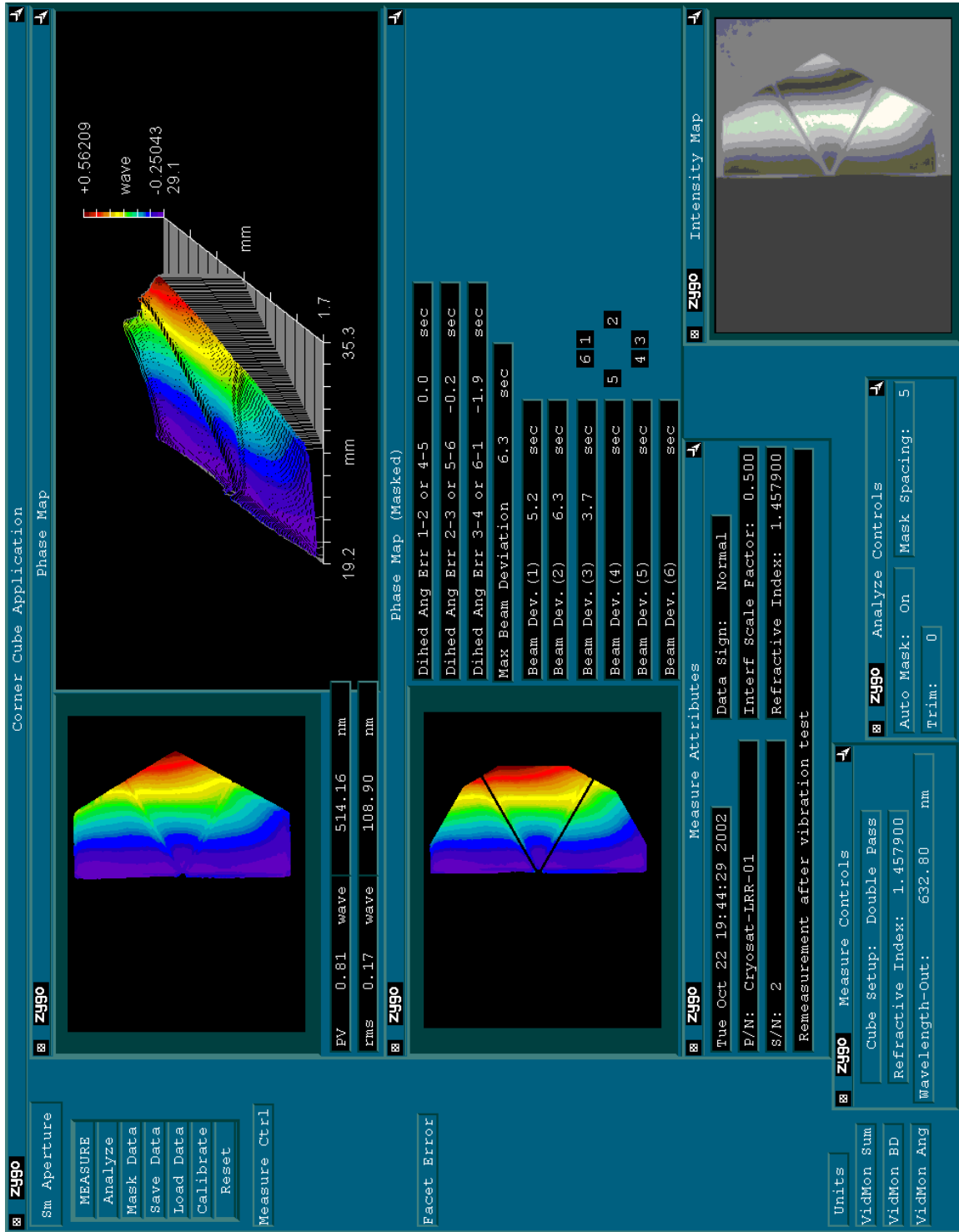


Fig. 5: Cryosat-LRR-01, cube #2, after vibration test

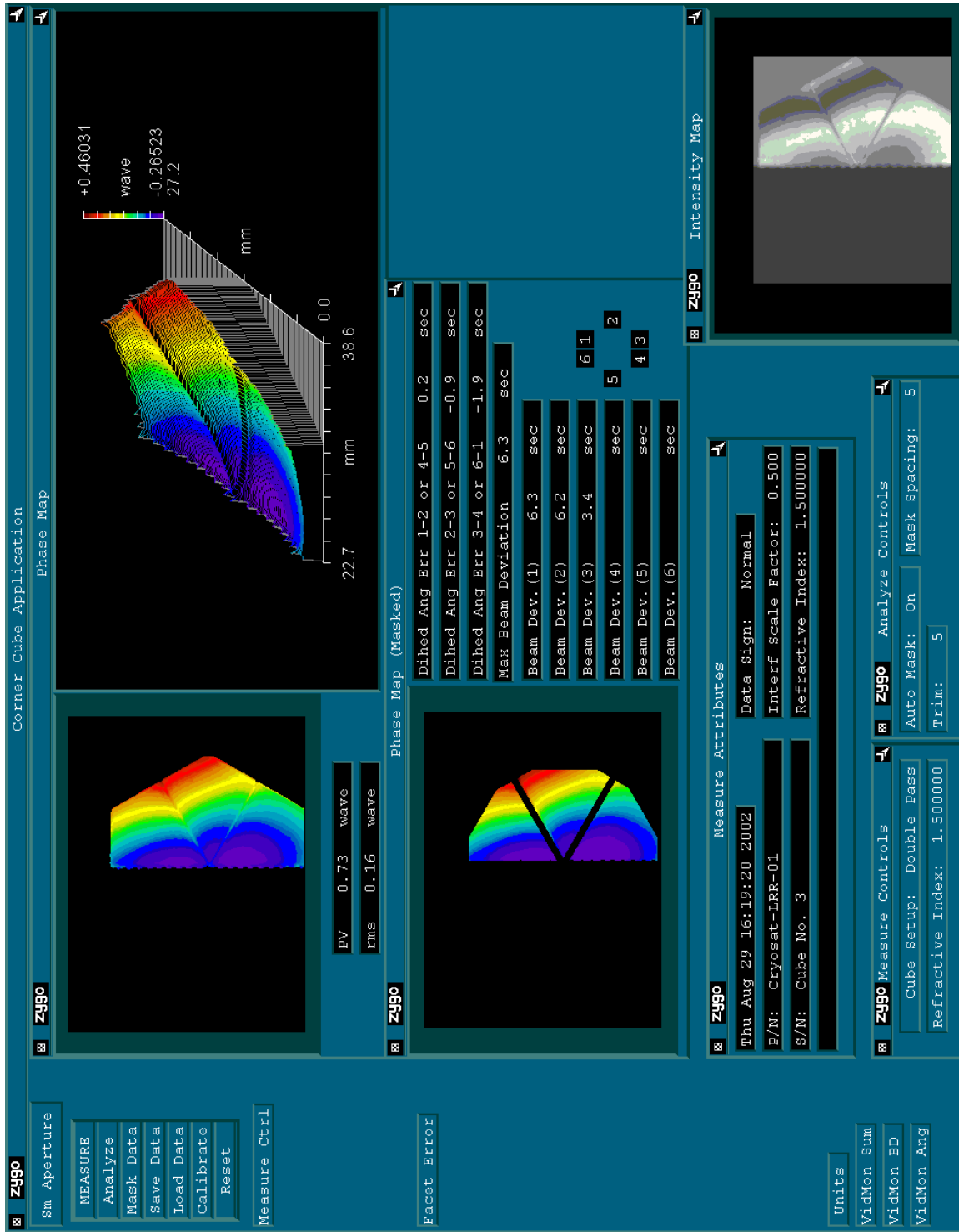


Fig. 6: Cryosat-LRR-01, cube #3, before vibration test

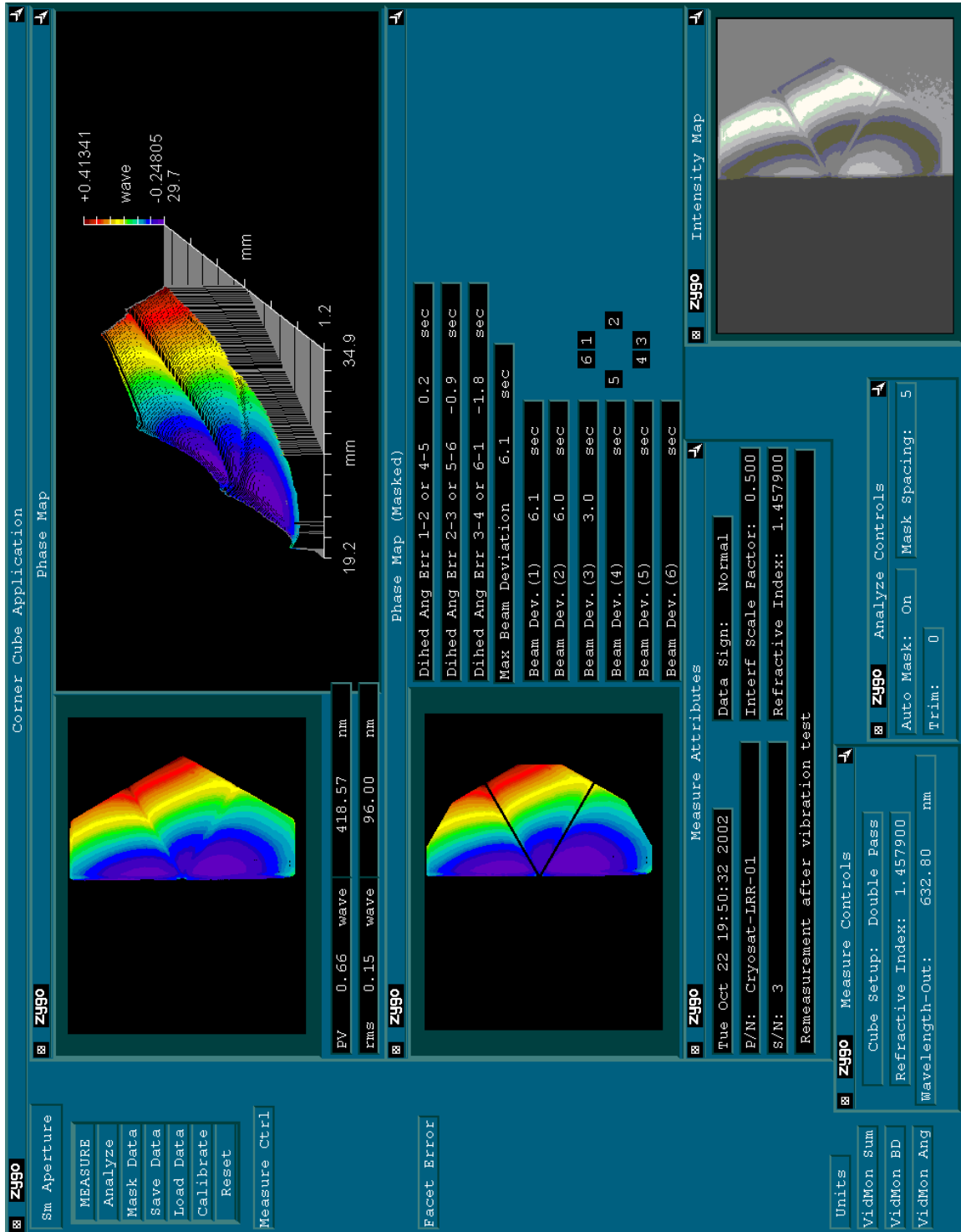


Fig. 7: Cryosat-LRR-01, cube #3, after vibration test

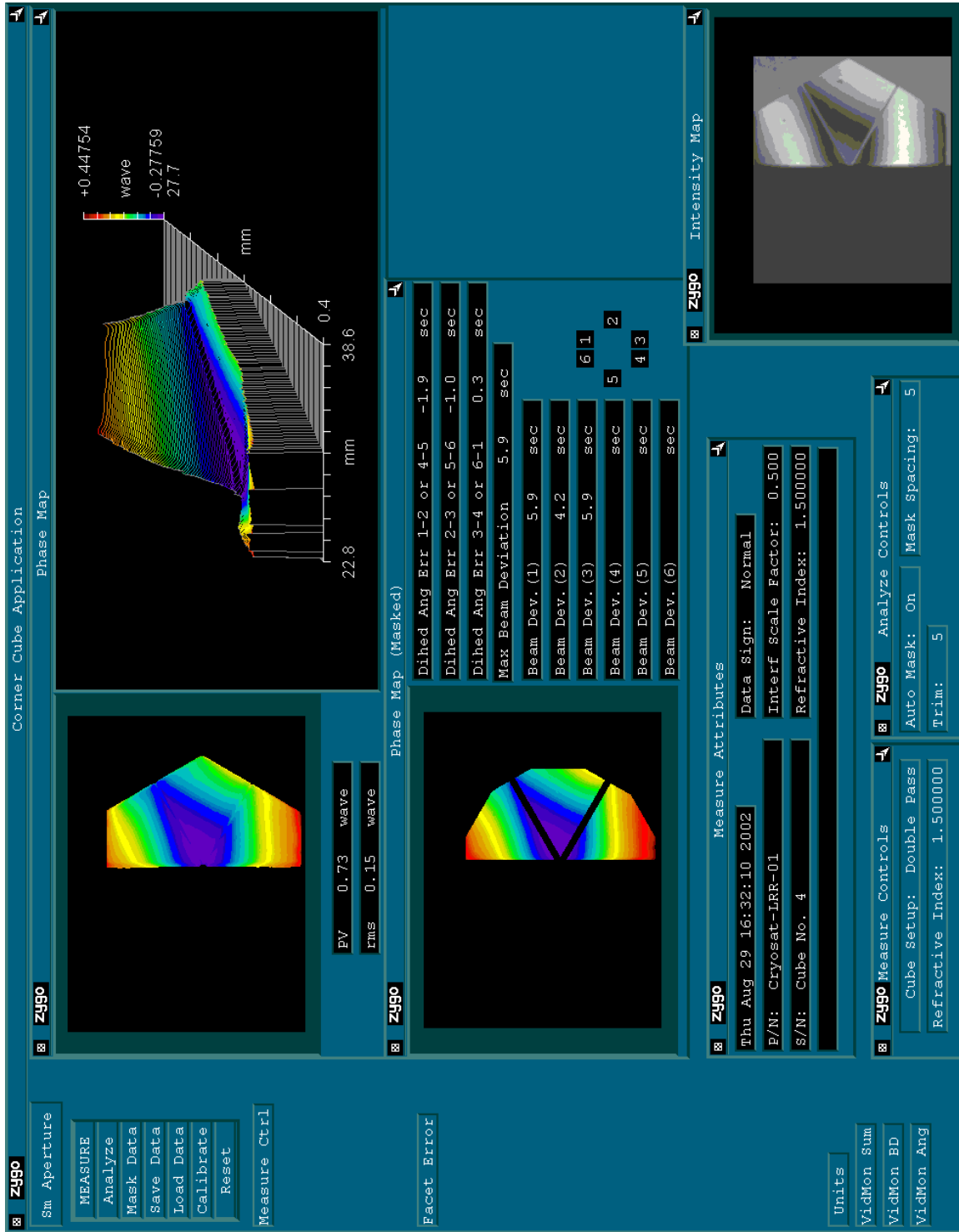


Fig. 8: Cryosat-LRR-01, cube #4, before vibration test

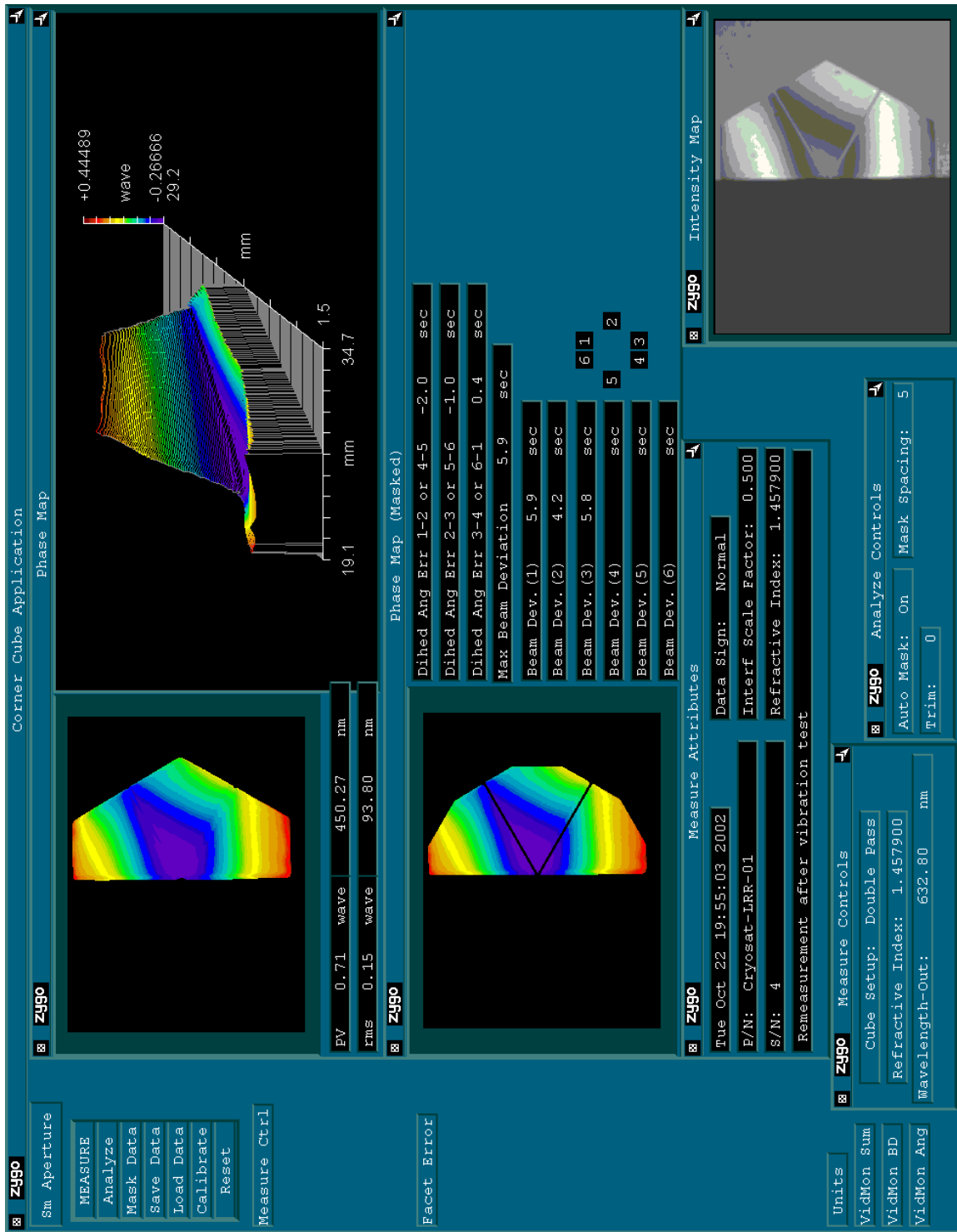


Fig. 9: Cryosat-LRR-01, cube #4, after vibration test

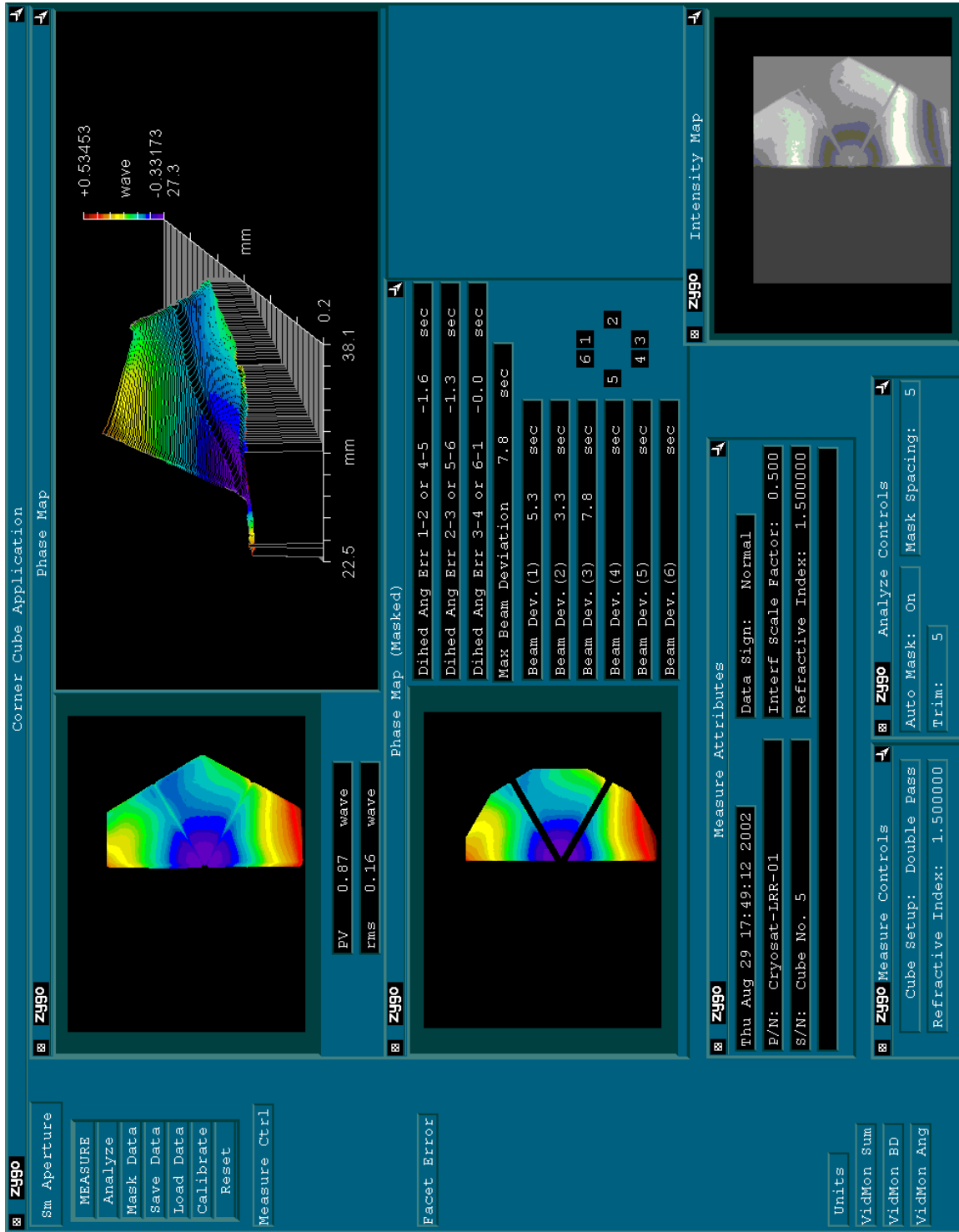


Fig. 10: Cryosat-LRR-01, cube #5, before vibration test

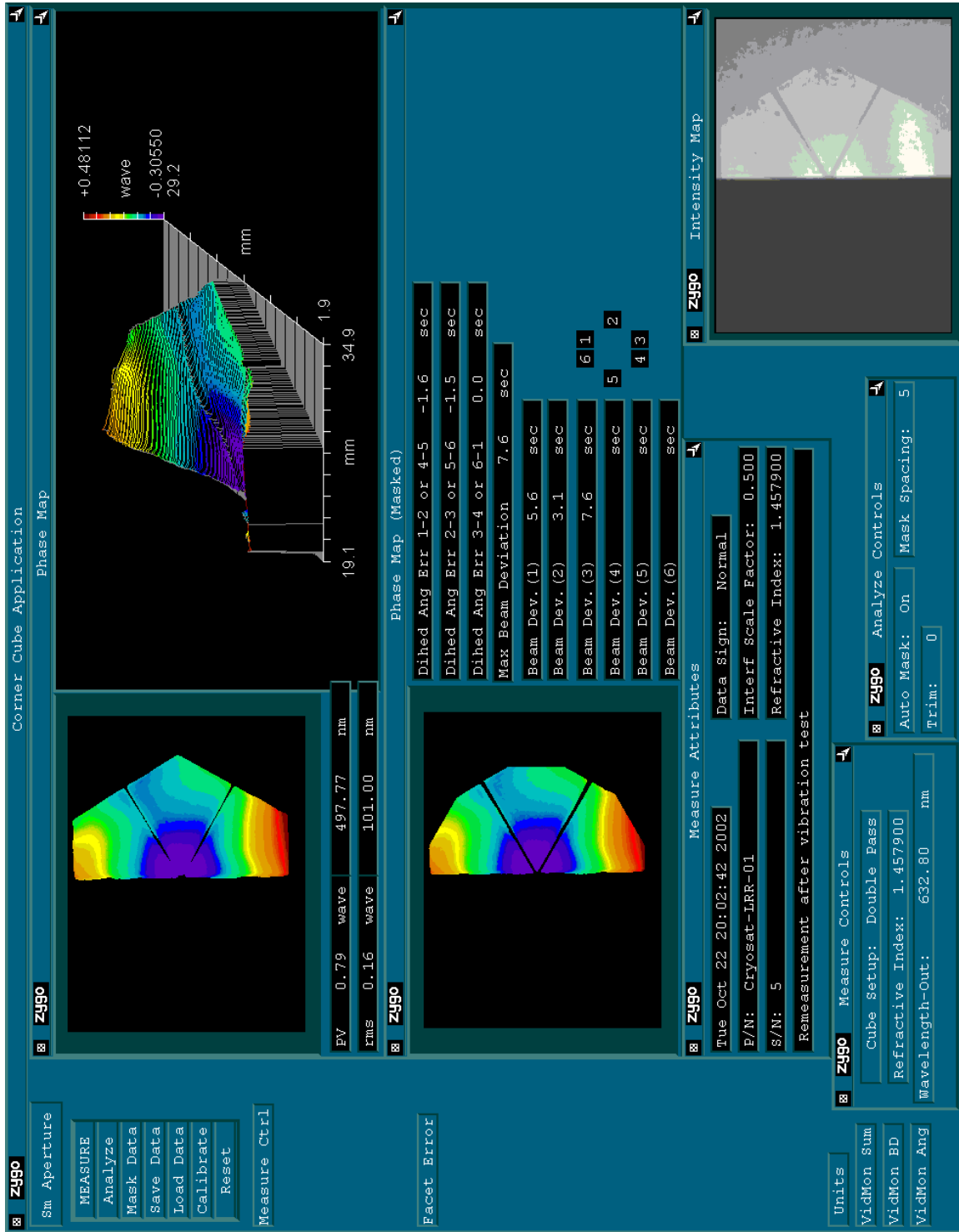


Fig. 11: Cryosat-LRR-01, cube #5, after vibration test

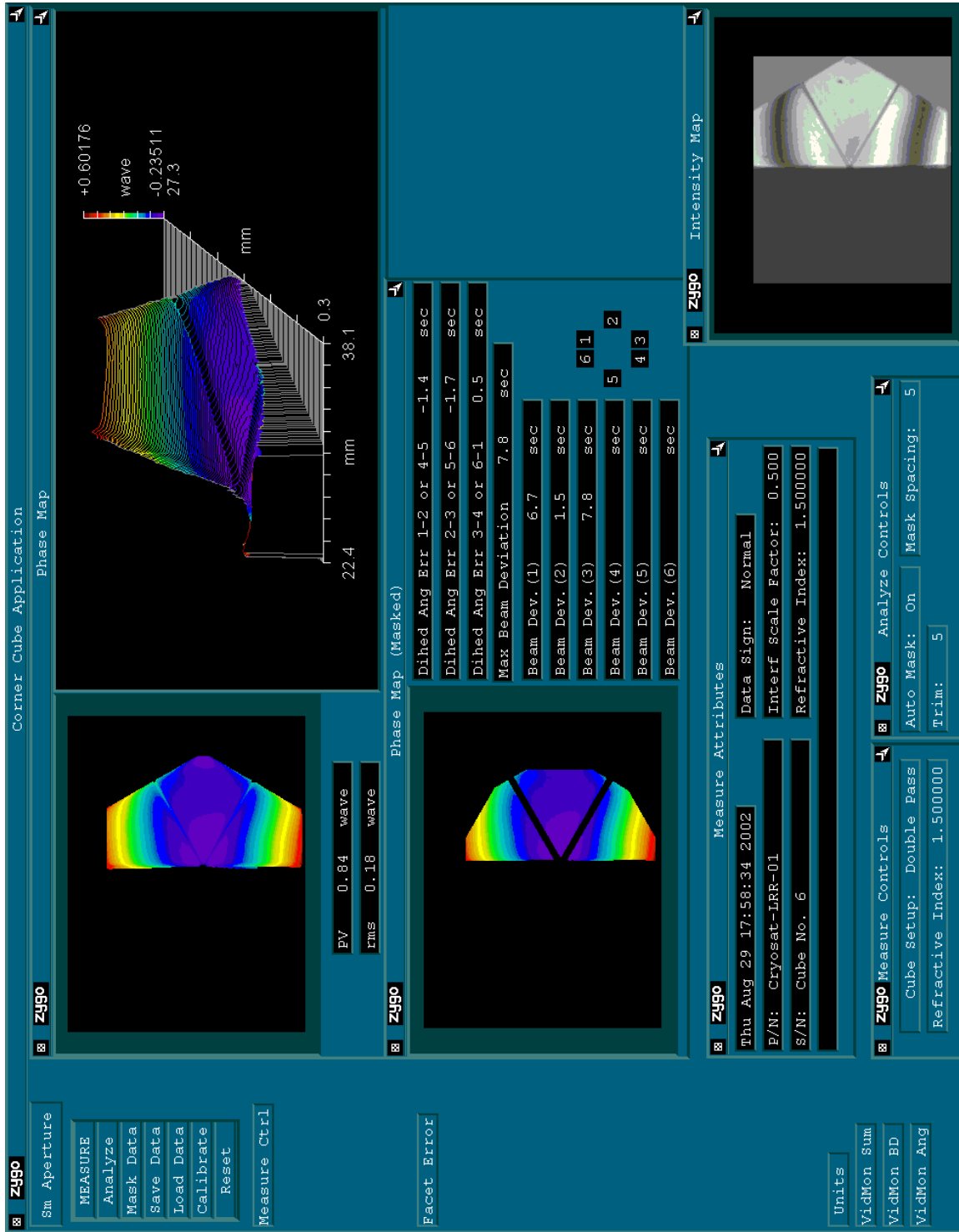


Fig. 12: Cryosat-LRR-01, cube #6, before vibration test

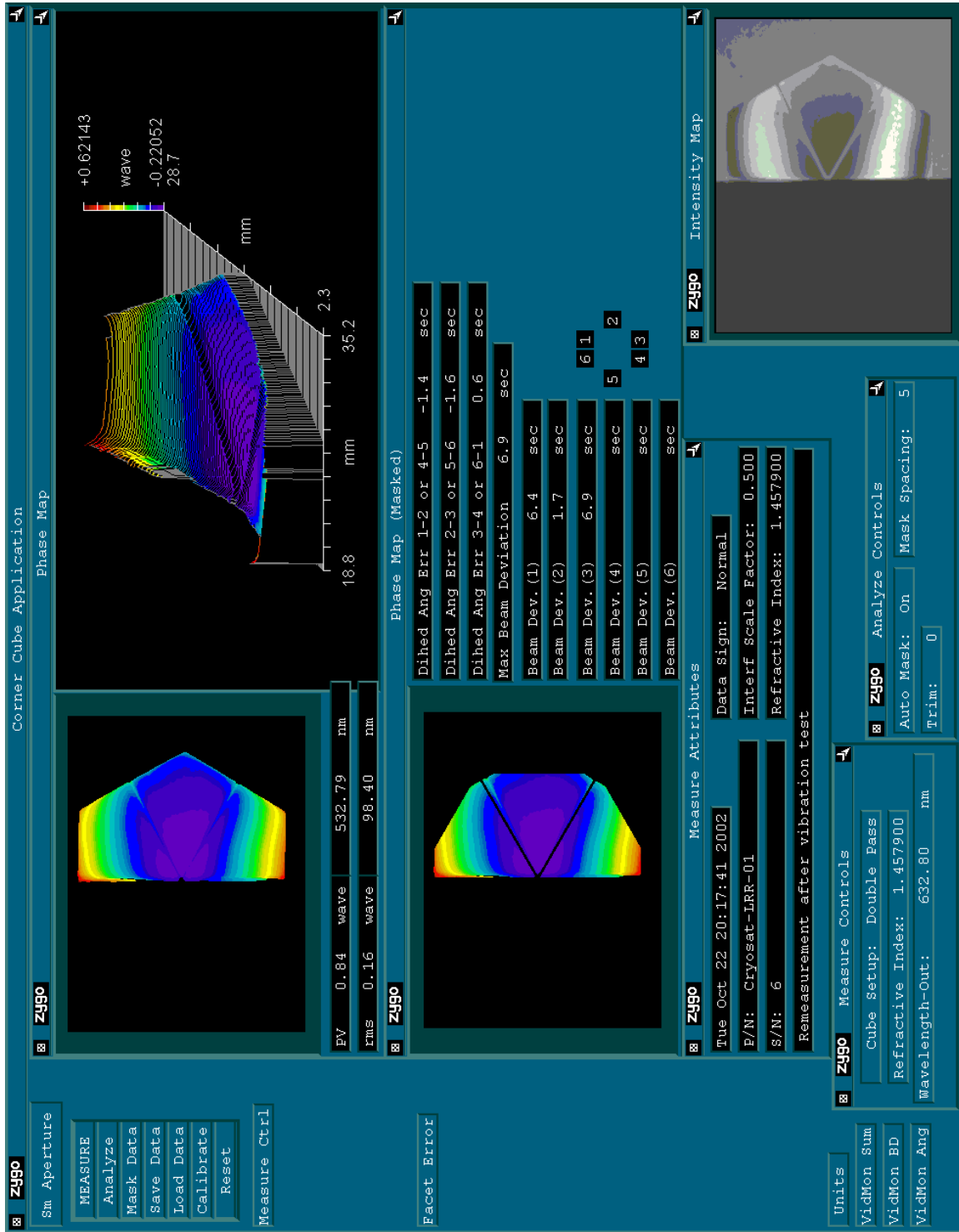


Fig. 13: Cryosat-LRR-01, cube #6, after vibration test

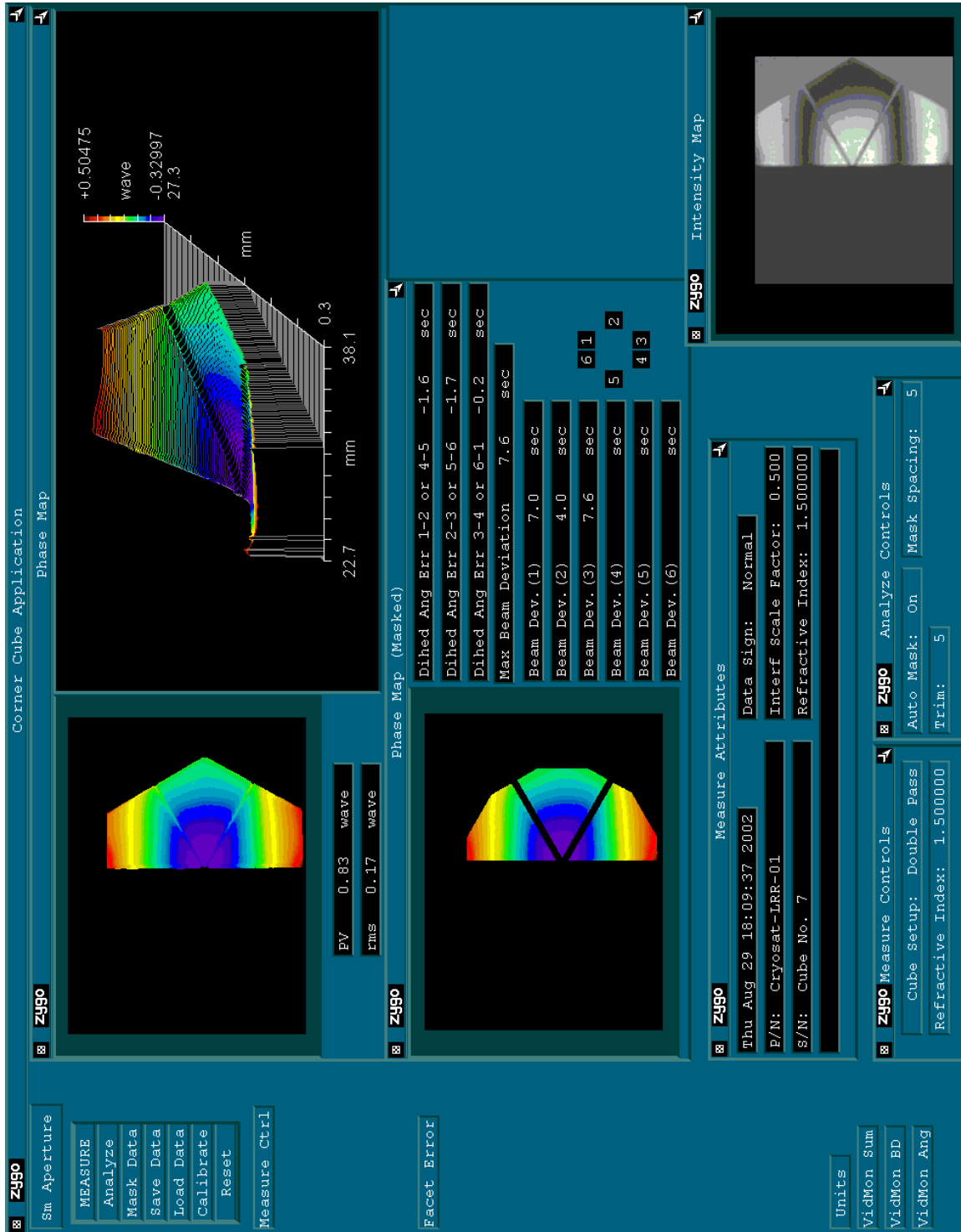


Fig. 14: Cryosat-LRR-01, cube #7, before vibration test

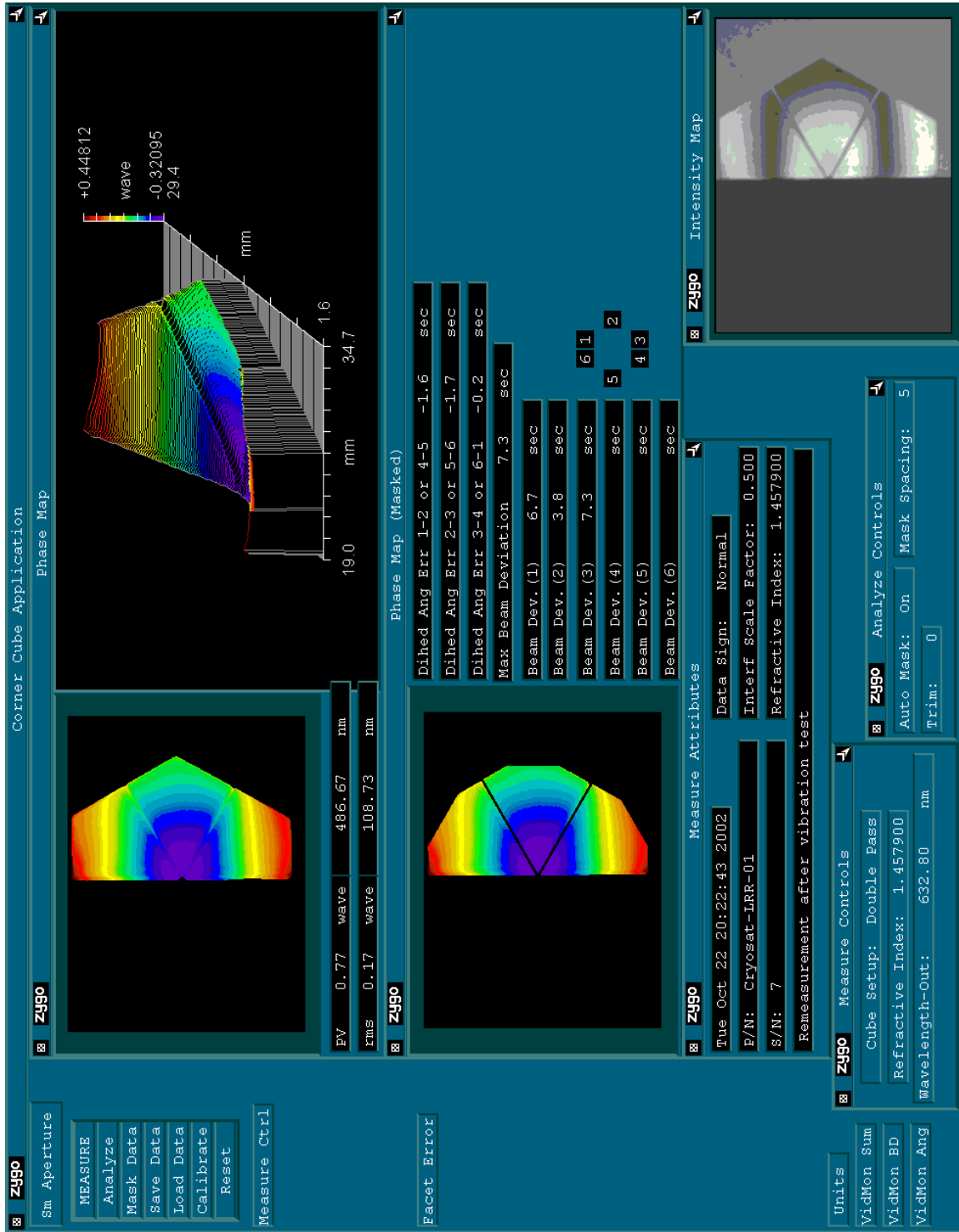


Fig. 15: Cryosat-LRR-01, cube #7, after vibration test